

Supporting Information

MOF-derived pyrrolic N-stabilized Ni single atom catalyst for selective electrochemical reduction of CO₂ to CO at high current density†

Jin Wook Lim^{1‡}, Dong Heon Choo^{2‡}, Jin Hyuk Cho^{3‡}, Jaehyun Kim⁴, Won Seok Cho¹, Odongo Francis Ngome Okello¹, Kiso Kim¹, Sungwon Lee¹, J. Son¹, Si-Young Choi¹, Jong Kyu Kim¹, Ho Won Jang^{4*}, Soo Young Kim^{3*}, and Jong-Lam Lee^{1,2*}

¹Department of Materials Science and Engineering, Pohang University of Science and Technology (POSTECH), Pohang 790-784 (Korea)

²Division of Advanced Materials Science, Pohang University of Science and Technology (POSTECH), Pohang 790-784 (Korea)

³Department of Materials Science and Engineering, Korea University, Seoul (Korea)

⁴Department of Materials Science and Engineering, Research Institute of Advanced Materials, Seoul National University, Seoul 08826 (Korea)

†Theses authors equally contributed to this work

*E-mail: jllee@postech.ac.kr

Keywords

Electrochemical CO₂ reduction, Ni single atom, pyrolysis, pyrrolic N, local configuration, flow cell

Experiment section

Synthesis of Ni ZIF-8

The metal-organic framework (MOF) structure of Ni/Zn zeolitic imidazolate framework-8 was fabricated by using a one-step solution-based process with vigorous stirring (denoted as Ni ZIF-8). First, 0.149g of $\text{Zn}(\text{NO}_3)_2 \cdot 6\text{H}_2\text{O}$ and 0.146g of $\text{Ni}(\text{NO}_3)_2 \cdot 6\text{H}_2\text{O}$ were dissolved in methanol. Then, a 0.7 M of 2-methylimidazole (2-MeIm) dissolved in methanol was poured into the mixed metal nitrate solution and vigorously stirred at room temperature for 24 h. Subsequently, Ni ZIF-8 powders were obtained by centrifugation (10,000 rpm, 15 min), thoroughly washed with methanol three times, and dried for 12 h under a vacuum at 80 °C.

Synthesis of Ni SAC

Ni single atom catalysts were prepared by a one-step pyrolysis process. For the heat treatment, a 0.5g of as-prepared Ni ZIF-8 powder was heated to 800 or 1000 °C at a rate of 25 °C/min and kept at the temperature for 4 h under the Ar atmosphere in a tube furnace, followed by naturally cooling down to room temperature. The pyrolysis products were denoted as Ni SAC. Depending on the pyrolysis temperature, the samples were denoted as Ni SAC-800, and Ni SAC-1000.

Characterization

Scanning electron microscopy (SEM) was performed using a field-emission scanning electron microscope (XL30S FEG, PHILIPS) with 5 kV acceleration voltage and 6 mm working distance. High-resolution transmission electron microscopy (HR-TEM) was conducted at 200 kV with Cs-corrector (JEOL JEM-2100). Atomic scale HAADF-STEM analysis was performed using a 200 kV operated S/TEM (JEOL ARM200F) with a spherical aberration corrector (ASCOR, CEOS GmbH, Germany). For HAADF imaging, the camera length was to

10 cm with inner and outer detector angles ranging between 45 – 180 mrad and probe size of 9C. Electron energy loss spectroscopy (EELS) elemental mapping was performed using JEM-2200FS at 200 kV. X-ray photoelectron spectroscopy (XPS) was performed using an X-ray photoelectron spectrometer (Thermo ESCALAB250i) with a monochromatic Al K α source ($h\nu = 1486.6$ eV) at a base pressure of 1×10^{-9} Torr. X-ray diffraction (XRD) patterns were recorded using a D/MAX-2500/PC (18 kW) (Rigaku) diffractometer with Cu-K α radiation ($\lambda = 0.15418$ nm) at 40 kV and 100 mA. The Ni metal contents were confirmed by inductively coupled plasma atomic emission spectrometry (ICP-AES) using iCAP 7400 (Thermo ScientificTM). The Raman spectra were obtained using a WITECH Alpha 300R Raman spectroscope equipped with a Nd:YAG laser. The excitation wavelength was 532 nm. X-ray absorption fine spectroscopy (XAFS) was performed in the transmittance and fluorescent detection mode in Pohang Accelerator Laboratory (PAL). The obtained XAFS data were analyzed using the ATHENA and ARTEMIS programs of the IFEFFIT package.

Electrochemical measurements

Cyclic voltammetry (CV), electrochemical impedance spectroscopy (EIS), electrochemical surface area (ECSA), Faradaic efficiency (FE), and current density were evaluated in a commercial microfluidic flow cell system (ElectroCell). Ag/AgCl filled with 3 M KCl was used for the reference electrode and a Pt plate was used for the counter electrode. Carbon paper (Sigracet 39 BB) coated with a microporous layer was used as a substrate for preparing the working electrode. The as-prepared catalyst powders (Ni ZIF-8 and Ni SAC) and 5 wt% nafion solution were ultrasonically suspended in ethanol to form a homogeneous catalyst ink. The catalyst ink was spray-coated onto the microporous layer of carbon paper with a size of 1.2 x 1.2 cm² and dried at 80 °C for more than 30 min (denoted as gas diffusion electrode (GDE)). The catalyst loading was 1 mg/cm². The anolyte and catholyte used for electrochemical

measurements were an aqueous solution of 0.5 M KHCO₃ (Sigma-Aldrich, 99.95%), which were separated by an ion exchange nafion membrane. Both electrolytes were cycled through each respective compartment at 50 ml/min. The CO₂ feed was supplied at the rate of 100 sccm to the back side of the carbon paper toward the catalyst layer. The measured potential ($V_{\text{Ag/AgCl}}$) could be converted to the reversible hydrogen electrode (V_{RHE}) using the Nernst equation: $V_{\text{RHE}} = V_{\text{Ag/AgCl}} + 0.222 + 0.0592 \times \text{pH}$. Gas products (H₂ and CO) were analyzed with gas chromatography (Inficon, 3000 Micro GC) equipped with two thermal conductivity detectors (TCD) connected to the Molsieve column and Plot U column. All the measurements were conducted under ambient pressure at room temperature.

DFT calculations

All DFT calculations were performed using Vienna ab initio simulation program (VASP version 6.2.1.) with projector-augmented wave (PAW) pseudopotentials and the revised Perdew–Burke–Ernzerhof (RPBE) exchange-correlation functional. A plane wave cutoff energy of 500 eV was used, and the convergence tolerances for energy and force were set to 10⁻⁴ eV and 0.05 eV Å⁻¹, respectively. The vacuum space of 20 Å was added to avoid nonphysical interactions between periodic images. A 2x2x1 Monkhorst-pack sampled k-point grid was employed to sample the reciprocal space for the models. To convert DFT-calculated total energies to Gibbs free energies, correction terms should be added, that is, $G = E_{\text{DFT}} + \text{ZPE} + \int C_p dT - TS + E_{\text{solv}}$, where E_{DFT} , ZPE, $\int C_p dT$, $-TS$, and E_{solv} correspond to the DFT-calculated energies, zero-point energies, enthalpic, entropic, and solvation corrections, respectively.

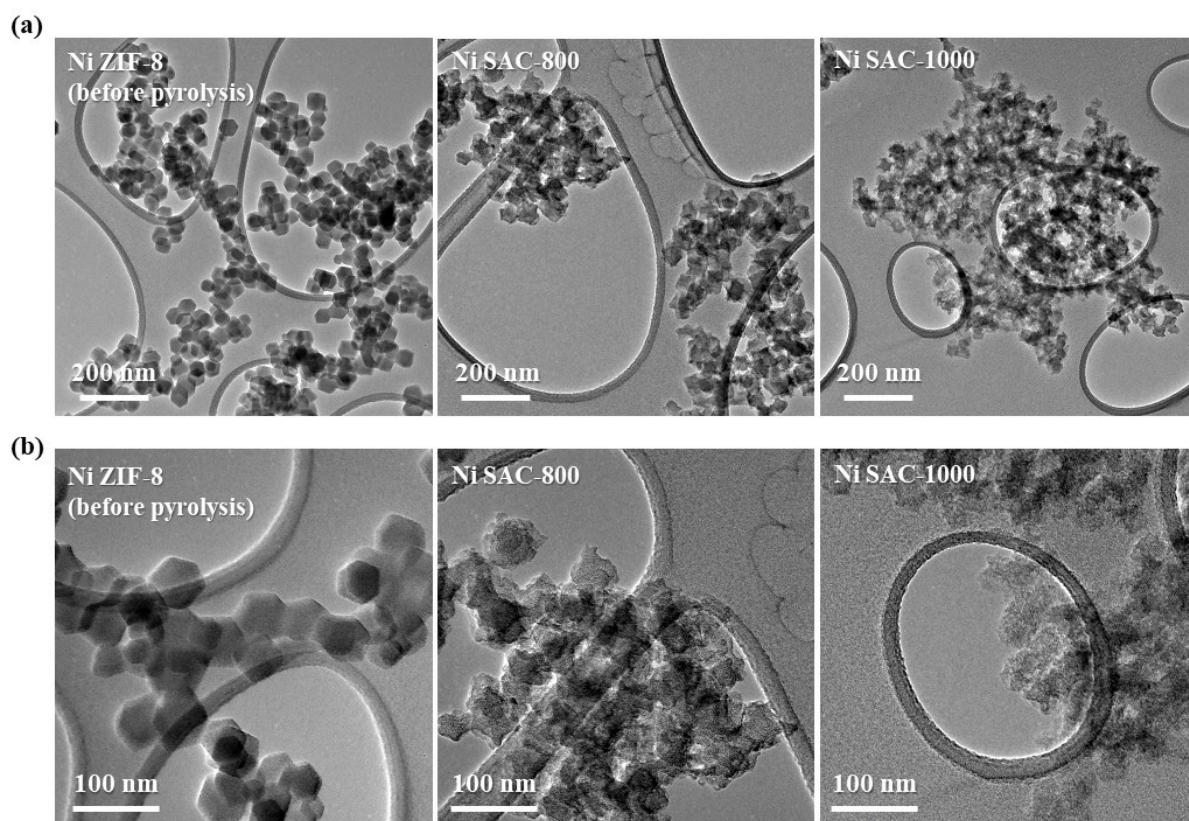


Fig. S1 HR-TEM images of Ni ZIF-8 (before pyrolysis), Ni SAC-800, and -1000 (after pyrolysis at 800 and 1000 °C).

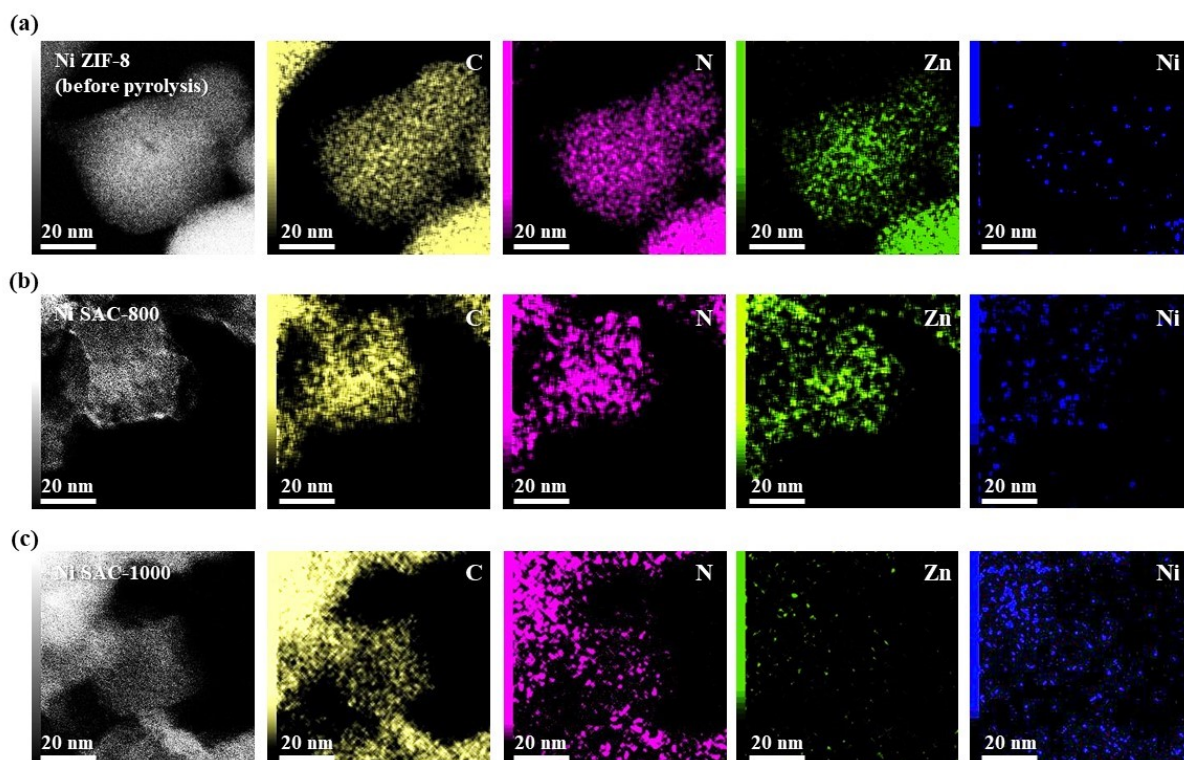


Fig. S2 TEM-EDS elemental mapping of C (yellow dot), N (purple dot), Zn (green dot), and Ni (blue dot) for Ni ZIF-8, Ni SAC-800, and -1000.

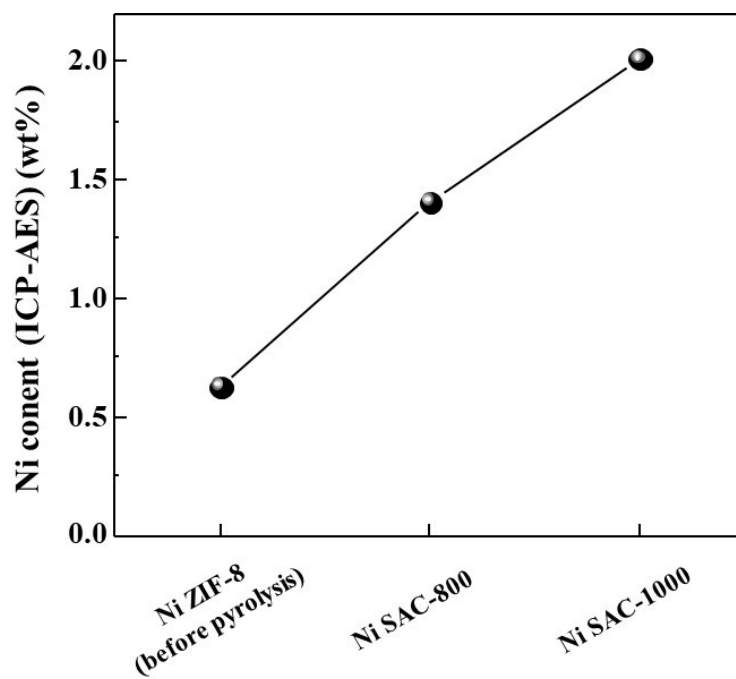


Fig. S3 Ni content (wt%) of Ni ZIF-8, Ni SAC-800, and -1000 as measured by ICP-AES.

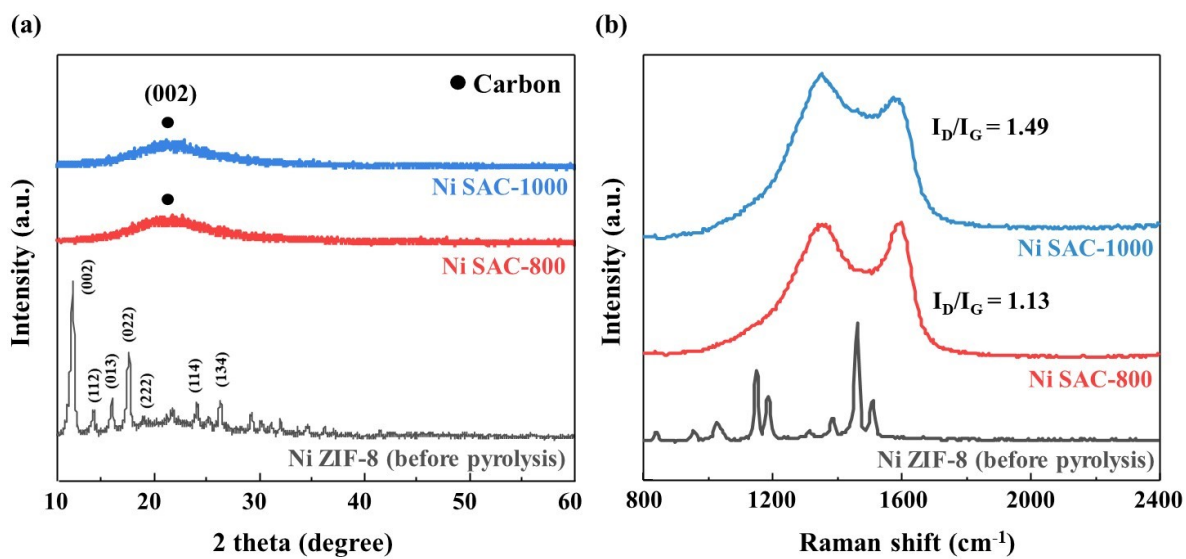


Fig. S4 XRD patterns and Raman spectra of Ni ZIF-8, Ni SAC-800, and -1000.

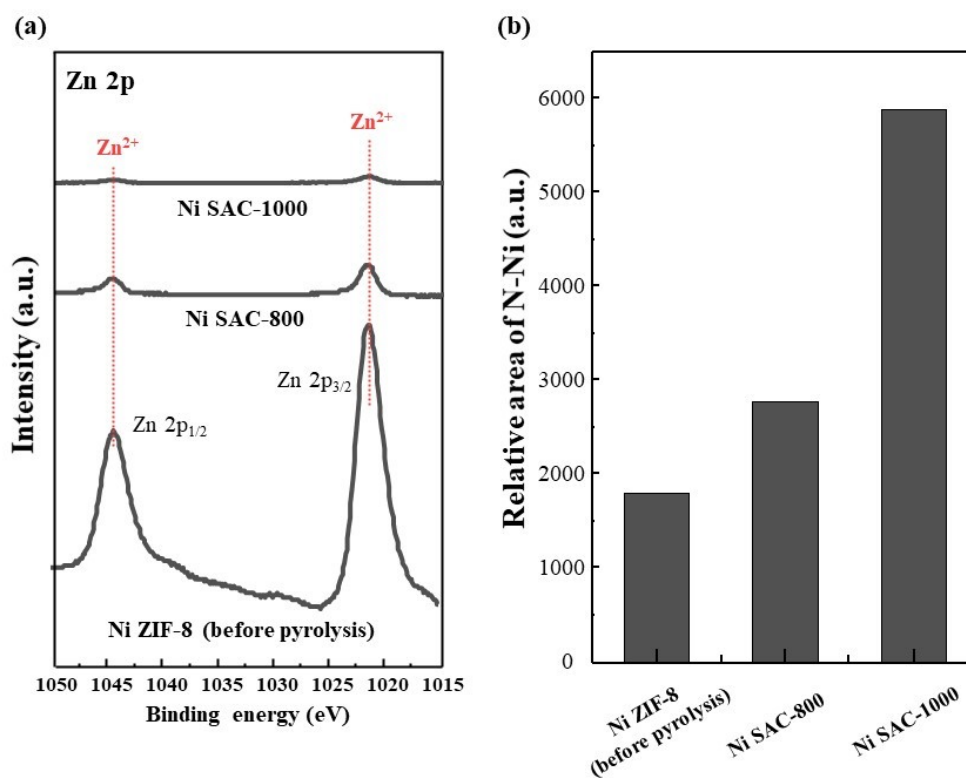


Fig. S5 Zn 2p XPS spectra of Ni ZIF-8, Ni SAC-800, and -1000 and relative area of N-Ni calculated by N 1s spectra.

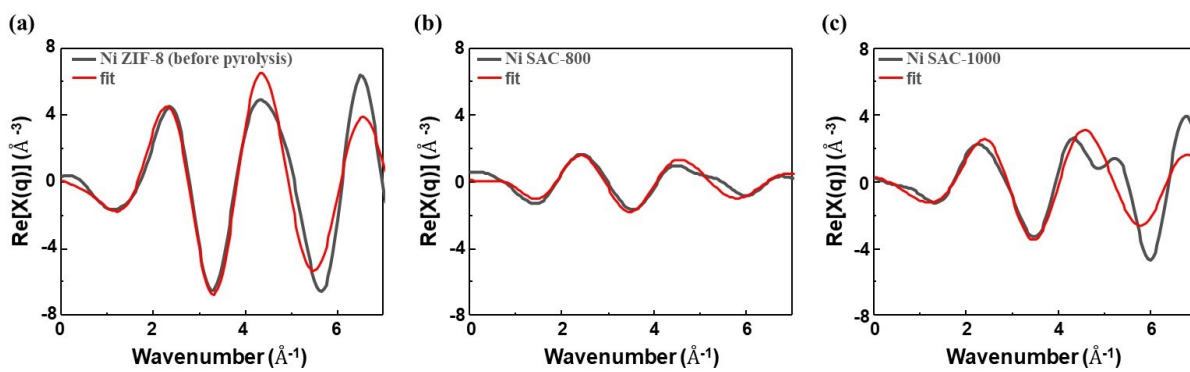


Fig. S6 EXAFS fitting curves of Ni K-edge for Ni ZIF-8, Ni SAC-800, and -1000 in k space.

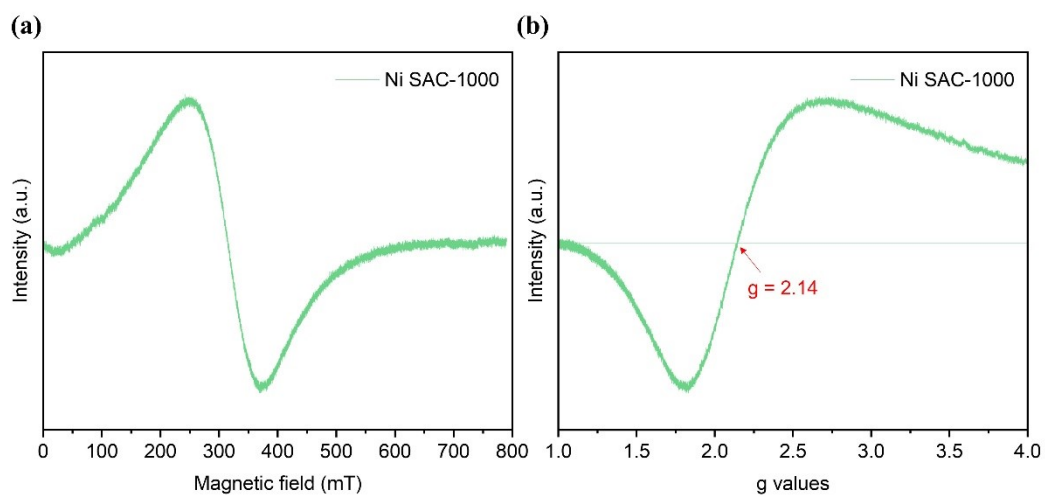


Fig. S7 Room-temperature EPR spectra of Ni SAC-100 at (a) magnetic field and (b) g-values.

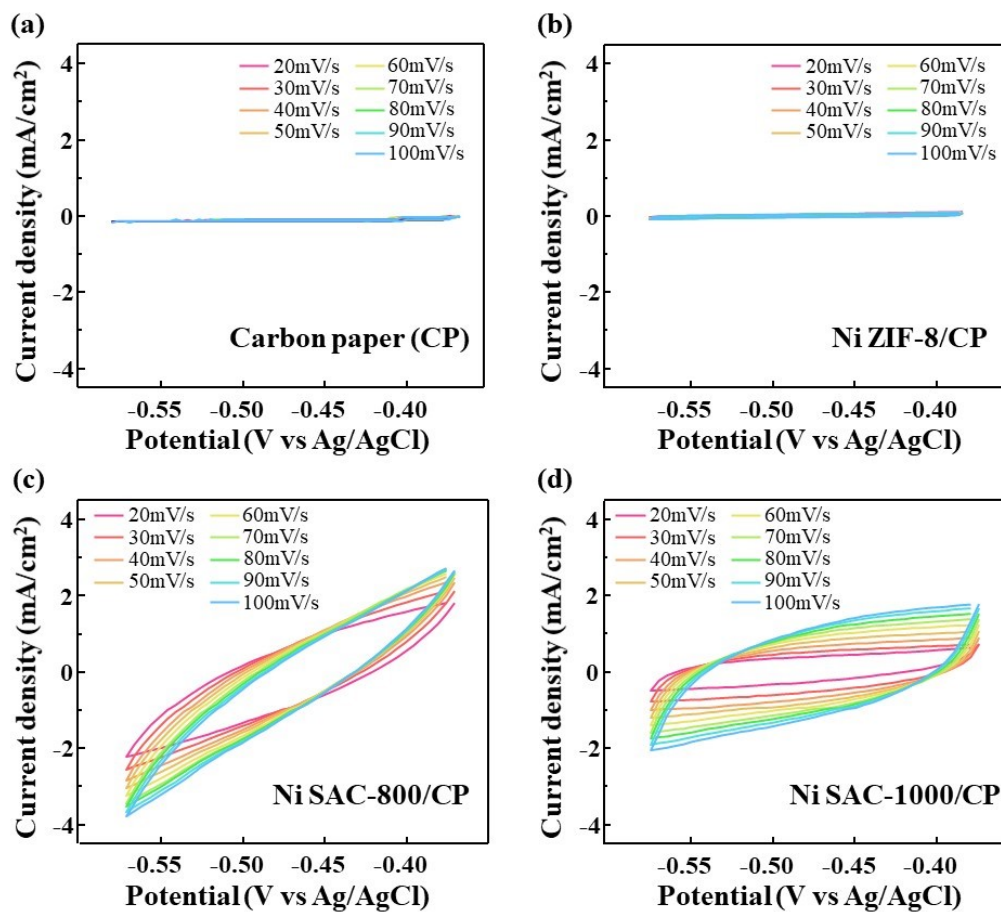


Fig. S8 Measured cyclic voltammetry on (a) carbon paper (CP), (b) Ni ZIF-8/CP, (c) Ni SAC-800/CP, and (d) Ni SAC-1000/CP with a potential range from -0.40 to -0.55 $V_{\text{Ag/AgCl}}$ in N_2 -purged 0.5 M $KHCO_3$.

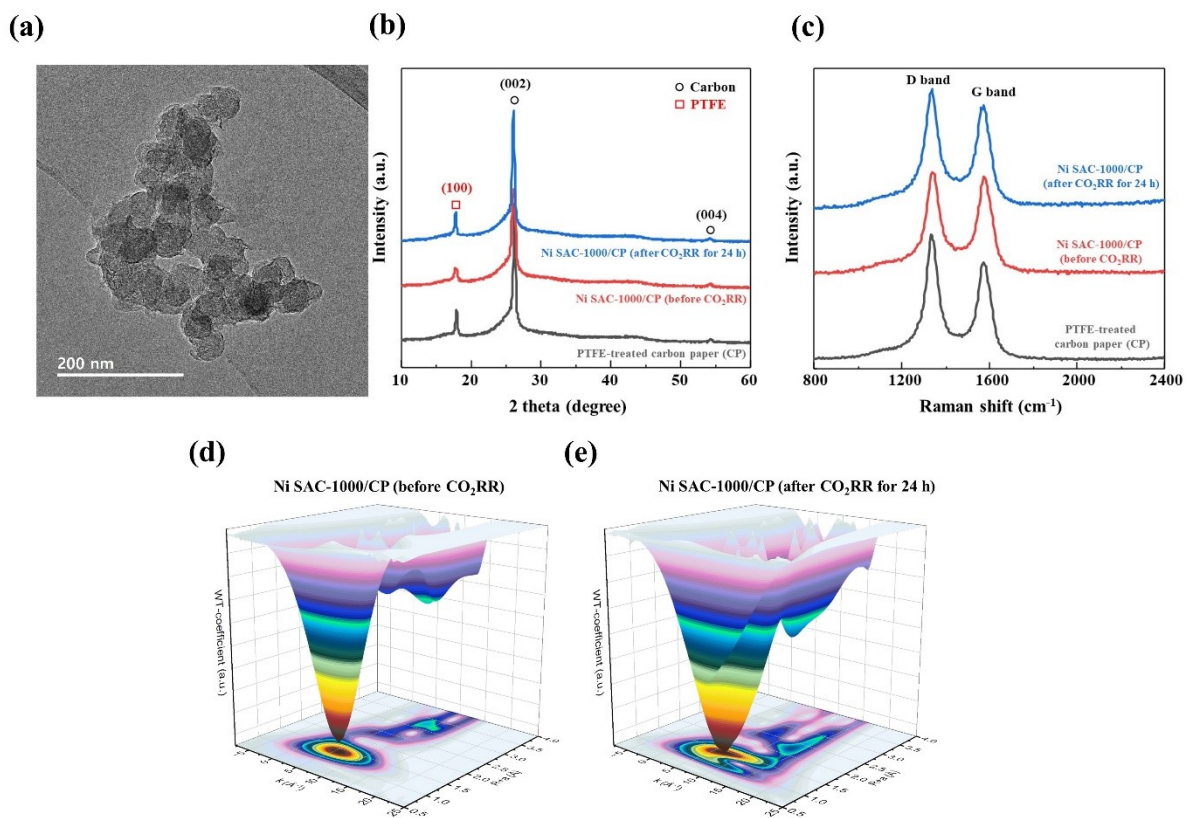


Fig. S9 TEM image, XRD patterns, Raman spectra and WT-EXAF data of PTFE-treated carbon paper (CP), Ni SAC-1000/CP (before CO₂RR), and Ni SAC-1000/CP (after CO₂RR for 24 h).

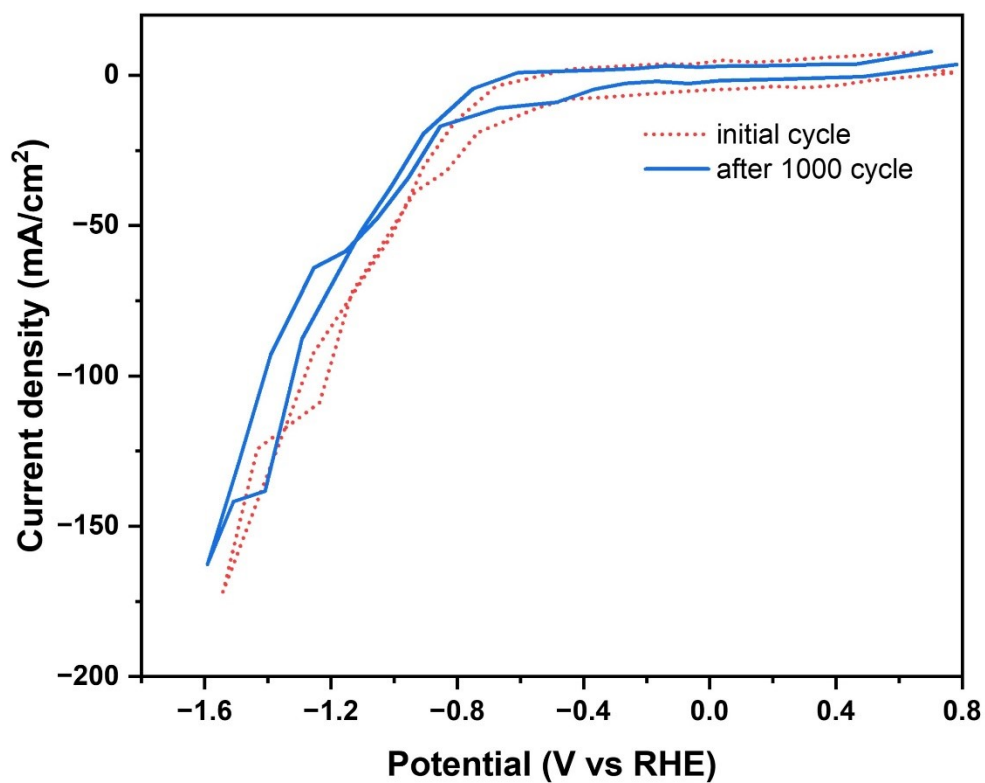


Fig. S10 Cyclic voltammetry (CV) curves of Ni-SAC-1000 during 1000 cycles of electrolysis in a microfluidic flow cell system in a CO₂-purged 0.5 M KHCO₃.

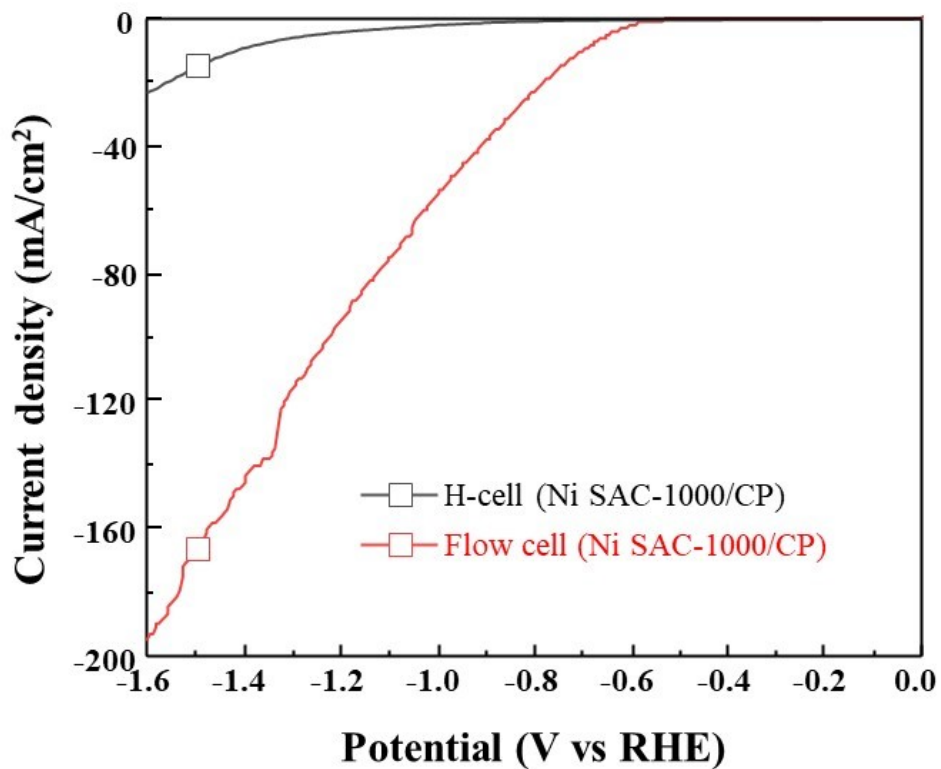


Fig. S11 LSV curves for Ni SAC-1000 were measured in a conventional H-type cell reactor and microfluidic flow cell system in CO₂-purged 0.5 M KHCO₃.

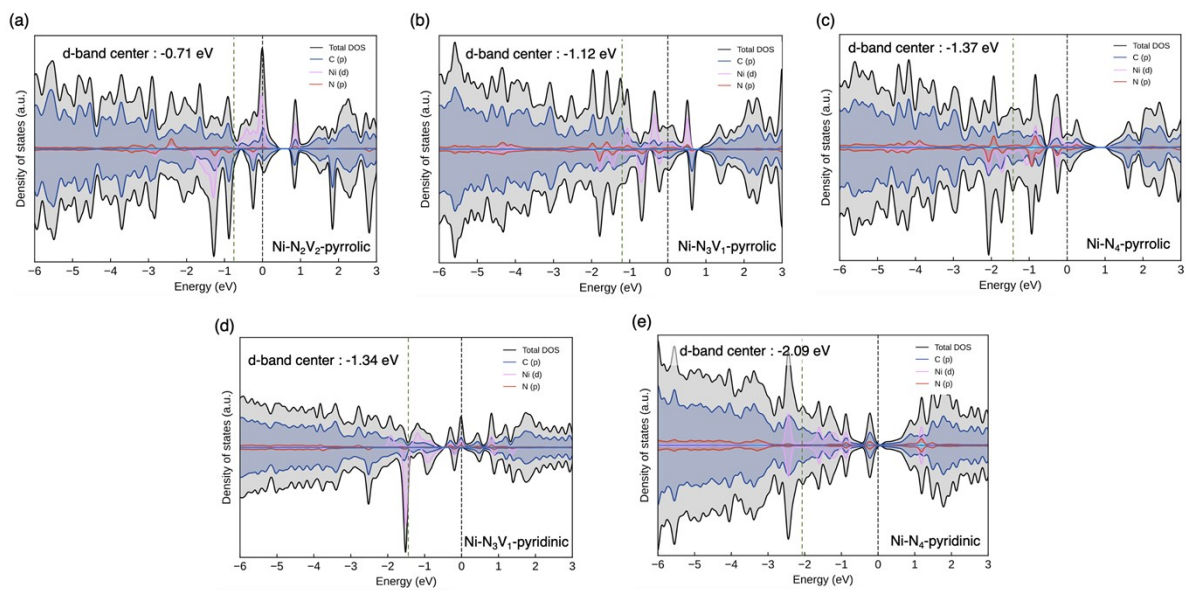


Fig. S12 Partial density of states of $\text{Ni-N}_x\text{V}_{4-x}$ with pyrrolic or pyridinic N coordination. (a) $\text{Ni-N}_2\text{V}_2$ with pyrrolic N, (b) $\text{Ni-N}_3\text{V}_1$ with pyrrolic N, (c) Ni-N_4 with pyrrolic N, (d) $\text{Ni-N}_3\text{V}_1$ with pyridinic N, and (e) Ni-N_4 with pyridinic N, respectively.

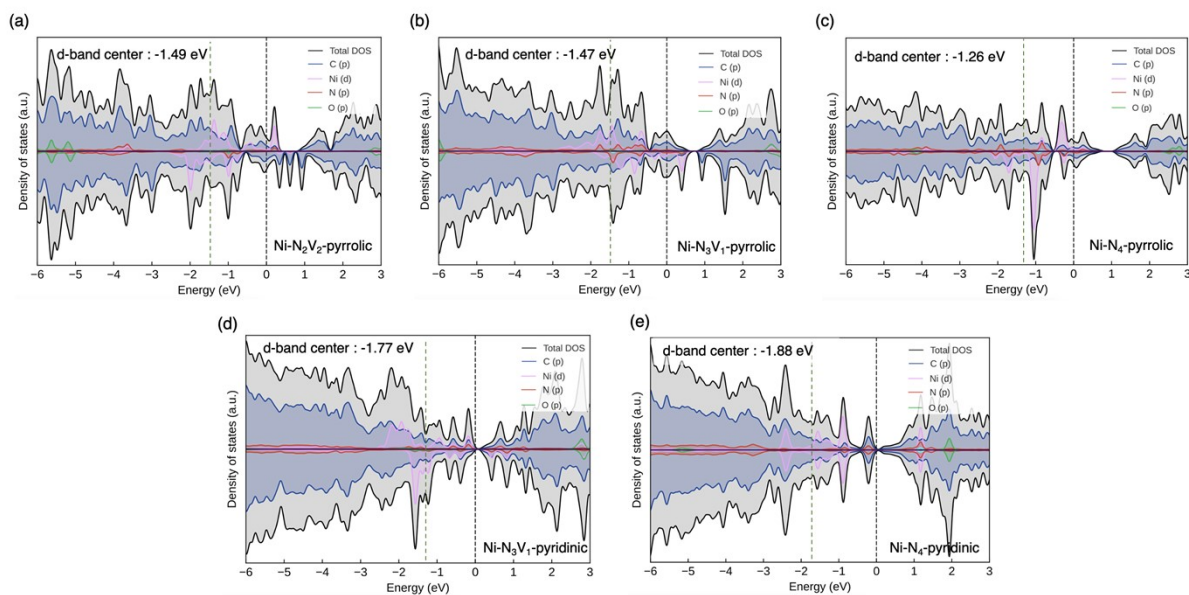


Fig. S13 Partial density of states of CO adsorbed Ni-N_xV_{4-x} with pyrrolic or pyridinic N coordination. (a) *CO@Ni-N₂V₂ with pyrrolic N, (b) *CO@Ni-N₃V₁ with pyrrolic N, (c) *CO@Ni-N₄ with pyrrolic N, (d) *CO@Ni-N₃V₁ with pyridinic N, and (e) *CO@Ni-N₄ with pyridinic N, respectively.

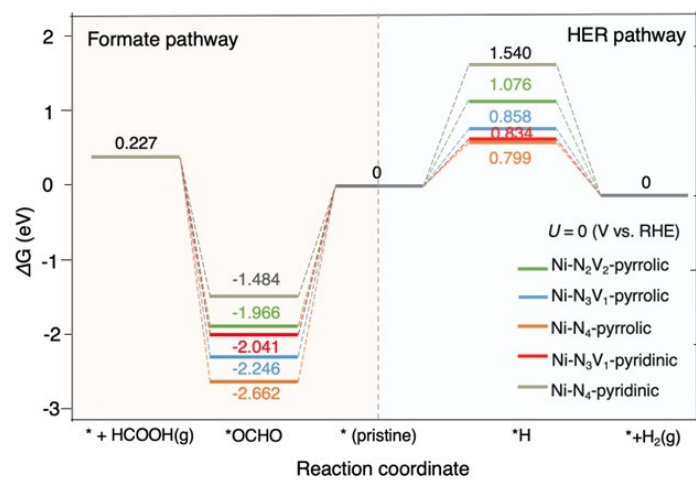


Fig. S14 Gibbs free energy diagram on electroreduction of CO₂ to formate pathway (left) and to hydrogen evolution pathway (right).

Table S1. Summary of measured pyrrolic N/pyridinic N ratio, Ni⁺/Ni²⁺ ratio, the relative area of N-Ni, and Ni content for as-prepared samples.

	Pyrrolic N/Pyridinic N ratio	Ni ⁺ /Ni ²⁺ ratio	Relative area of N-Ni (XPS)	Ni content (ICP-AES)
Ni ZIF-8 (before pyrolysis)	0	0	1812.25	0.63 wt%
Ni SAC-800	0.3768	1.7847	2765.51	1.41 wt%
Ni SAC-1000	1.0195	2.2574	5881.07	2.01 wt%

Table S2. Summary of measured D and G band intensity and relative I_D/I_G ratio for Ni ZIF-8, Ni SAC-800, and Ni SAC-1000.

	Intensity (D band)	Intensity (G band)	I_D/I_G ratio
Ni ZIF-8 (before pyrolysis)	Not detected	Not detected	-
Ni SAC-800	118.40	104.37	1.13
Ni SAC-1000	143.12	96.02	1.49

Table S3. The local structure environment of coordination number, and bond distance for as-prepared samples calculated by EXAFS fitting results.

Catalysts	Bond	Coordination number (CN)	Bond distance, R (Å)
Ni foil	Ni-Ni	12	2.20
Ni Pc	Ni-N	4	1.78
Ni ZIF-8 (before pyrolysis)	Ni-N	4	1.78
Ni SAC-800	Ni-N	3.14	1.71
Ni SAC-1000	Ni-N	2.63	1.60

Table S4. Comparison of catalytic performance for as-prepared samples in CO₂-purged 0.5 M KHCO₃.

As-prepared samples	Potential (V _{RHE})	FE _{H₂} (%)	FE _{CO} (%)	<i>j</i> _{H₂} (mA/cm ²)	<i>j</i> _{CO} (mA/cm ²)
Carbon paper (CP)	-0.4	3.40	0	0.01	0
	-0.6	11.82	0	0.07	0
	-0.8	37.16	0	2.78	0
	-1.0	32.30	0	2.10	0
	-1.2	76.44	0	21.25	0
	-1.4	34.68	0	12.91	0
Ni ZIF-8/CP (before pyrolysis)	-0.4	12.50	0	0.80	0
	-0.6	25.70	0	1.10	0
	-0.8	45.32	0	3.09	0
	-1.0	21.74	0	1.98	0
	-1.2	42.60	9.50	5.73	2.91
	-1.4	41.52	4.23	7.14	1.57
Ni SAC-800/CP	-0.4	2.89	20.50	0.05	0
	-0.6	13.30	34.82	0.42	1.28
	-0.8	28.90	40.76	2.24	2.70
	-1.0	51.16	25.03	7.08	2.49
	-1.2	68.87	18.58	21.49	2.36
	-1.4	68.88	11.49	40.64	4.41
Ni SAC-1000/CP	-0.4	4.13	79.79	0.10	1.36
	-0.6	3.13	87.32	0.19	4.86
	-0.8	2.07	98.24	0.39	45.03
	-1.0	1.60	95.03	0.96	59.38
	-1.2	1.98	98.09	1.98	108.35
	-1.4	2.46	95.11	3.51	148.25

